2nd IFAC Workshop on Research, Education and Development of
Unmanned Aerial Systems
November 20-22, 2013. Compiegne, France

Switching algorithm for data fusion of small low-cost UAV navigation system ⋆

Boris Andrievsky *,**,**** **Nikolay V. Kuznetsov** *,***
Olga A. Kuznetsova * **Gennady A. Leonov** *

* *Saint-Petersburg State University, 28 Universitetsky prospekt, 198504, Peterhof, Saint Petersburg, Russia, leonov@math.spbu.ru, kuznetsov@math.spbu.ru, o_a_kuznetsova@mail.ru*
** *Institute for Problems of Mechanical Engineering, the Russian Academy of Sciences, 61 Bolshoy prospekt, V.O., 199178 Saint Petersburg, Russia, boris.andrievsky@gmail.com*
*** *Department of Mathematical Information Technology, University of Jyväskylä, PO Box 35, FI-40014, Finland*
**** *Saint Petersburg National Research University of Information Technologies, Mechanics and Optics, Russia*

Abstract: The switching algorithm for fusion data of satellite navigation system and standard onboard sensors for low-cost unmanned aerial vehicle (UAV) is proposed and numerically studied by the example of the hypothetical small jet-propelled UAV.
Keywords—sensor data fusion, UAV dynamics, control, guidance, navigation

1. INTRODUCTION

The sole Global Navigation Satellite System (GNSS) system cannot provide the UAV navigation system with all the data necessary for guidance. The relatively low data rate and possible loss of the signals from satellites can be mentioned among the GNSS demerits. This causes the lack of the GNSS navigation continuity (Strachan, 1997; Tanju et al., 2000; Mutuel and Speyer, 2000; Blomenhofer, 1996–1997). The typical and the most undeniable solution lies in the data fusion of the GNSS and the onboard Integrated Navigation System (INS). For data processing of the GNSS/INS navigation systems, the Kalman filtering is commonly used. In the present paper we consider applicability of an alternative approach for a small low-cost air vehicle navigation, assuming absence of the onboard INS. Continuity requirement is ensured by means of the Kalman filtering and customary onboard sensors. The Kalman estimator receives data from the airborne sensors (gyros, accelerometers, altitude sensor, etc.) and provides the guidance system with the high-rate state estimates of the UAV (i.e. with the rate, which is required for guidance and control along the trajectory). The GNSS signals are used for renewing the estimates at the instants (possibly random) of GNSS availability. The sample time of renewing may significantly exceed the sample time, used for Kalman filtering. Typically, only the models of sensors and GPS/INS errors (Vallot et al., 1991; Coffee and Maganty, 1996) are used for Kalman filtering in GNSS/INS navigation systems. It is worth mentioning that in the series of papers, devoted to navigation of autonomous aerial, underwater and ground vehicles, the vehicle dynamics are taken into consideration for enhancement the existing INS performance (Dmitriev et al., 1999; Koifman et al., 1995; Koifman and Bar-Itzhack, 1999; Algrain and Saniie, 1994; Perera et al., 2010; Hegrenaes and Hallingstad, 2011; Sazdovski and Silson, 2011; Vasconcelos et al., 2011, 2010; Morgado et al., 2013). In our study it is assumed that no onboard INS is present. To use the proposed method, more detailed and accurate UAV dynamics model than commonly used for GNSS/INS Kalman filtering is needed. It should be mentioned that the present method is not suggested as a way for navigation precision enhancement comparing with combined GNSS/INS navigation systems. The purpose of the present research is to find out what a level of precision can be ensured by the purely algorithmic means, without employing the onboard INS.

⋆ Partially supported by the Saint Petersburg State University, Academy of Finland, the Russian Foundation for Basic Research (grant Nos. 12-08-0118, 13-08-00925, 13-08-01014), Grant of RF President No MK-3133.2012.1 and the Russian Federal Program "Cadres" (agreements 8846, 8855).

2. UAV NAVIGATION METHOD USING GNSS AND KALMAN ESTIMATOR

2.1 System Structure and Principal Parameters

Consider the small-size UAV, equipped with the following sensors: the GNSS receiver; the gyro-sensors for Euler angles (pitch angle ϑ, yaw angle ψ, roll angle γ) measurement [1]; the rate gyros measuring the angular velocities with respect to the body-fixed reference frame (ω_x, ω_y, ω_z); the barometric altimeter; the g-meters measuring accelerations along the axes of the body-fixed frame (j_x, j_y, j_z); the rudders deflection sensors (δ_e, δ_r, δ_a); the onboard computer

[1] The Russian notations are used in this paper. They differ from those of the ISO 1151-5 standard.

for primary and secondary navigation data-processing, flight path tracking and control; the steering gears and the auxiliary equipment. UAV has four controlling inputs: the symmetrical and differential taileron deflection (δ_a, δ_e), the rudder deflection (δ_r), and the engine throttle (thrust position δ_{th}).

The key problem, considered in the paper is fulfilment of the GNSS and the sensors data fusion. Preliminary data processing the GNSS signals is realized by means of the separate algorithm and is not considered here.It is assumed that this algorithm converts the pseudorange measurements from the GNSS receiver into the estimates of UAV position in a certain Earth-fixed frame (x, h, z) and UAV velocity with respect to the Earth (V_k). These data are used for renovation of the Kalman estimates at time instants $\{t_K\}$. Below, for the numerical analysis, that $t_K = K \cdot T_S$ $(K = 0, 1, 2, \ldots)$ is taken, where T_S is a sampling time which is assumed to be noticeably greater that of the Kalman estimator (denoted below as T_s), $T_S \gg T_s$. For distinctness, $T_S = 5$ s is taken. The value T_S is not used for the estimator algorithm design, therefore the case when the instants $\{t_K\}$ are not equally spread is also possible: $t_K = t_{K-1} + T_S(K)$, say, with the random increments $T_S(K)$.

In the present study, without loss of generality, it is assumed that the sensor data flow, Kalman estimation and the controlling signals have the equal sample rate $f_s = 1/T_s$. Typically, $f_s = 40 \div 100$ Hz. Sample time T_s in 20 ms (i.e. $f_s = 50$ Hz) is chosen hereafter.

3. ESTIMATOR DESIGN

The process of the estimator design has several phases. Firstly, the linearized UAV model is obtained. Secondly, the extended model, including the model of some disturbances is obtained. Thirdly by means of the discretization on time with given sample period T_s the discrete-time extended model is found. This leads to the *switched* navigation algorithm (Tanwani et al., 2013; Balluchi et al., 2012). The Kalman-estimator design technique is applied to this model and the discrete-time estimator equations are finally obtained. More detailed description of this procedure is given below.

The UAV dynamics are nonlinear and depend on the flight conditions (the flight velocity V, the altitude h, the path angle θ and some other factors) (Hemsch and Mendenhall, 1992). Immediate design of discrete-time Kalman estimator for a time-variant nonlinear system is a very challenging problem and can lead to algorithms, which are difficult for implementation and performance analysis. Therefore, it is seems reasonable to apply more simple and rough design technique based on the linear approximation of the plant dynamics. The quality of the obtained solution should be inquired subsequently with usage of the initial (nonlinear) model. For estimator design and the numerical study of the navigation system the UAV dynamics model presented in (Chen et al., 2009; Ye et al., 2006) is employed in the paper.

Extended UAV model involves the UAV dynamics equations and the internal model of disturbances (where measuring errors: position, velocity, attitude errors, gyro drift, accelerometer bias, etc. can be added). In the present study only the wind disturbances are included into the extended model, more specifically, the systematic components of the wind velocity vector $W = \mathrm{col}\{W_x, W_y, W_z\}$ is taken into account. Assuming they are constant, one gets the following internal model of disturbances:

$$\dot{W}_x = 0, \quad \dot{W}_y = 0, \quad \dot{W}_z = 0. \tag{1}$$

Two extended UAV models are used below. The first one ("Model-I") is suggested as a constituent of the real-time estimation algorithm, and the next one ("Model-II") is intended for the estimator design. Let us describe them in details.

The numerical analysis and simulations show that the considered system with the vector y_I as an output is ill-conditioned in the sense of observability with respect to $V_k(t)$ and $\Psi(t)$. Therefore, the estimates of these state variables are highly sensitive to the disturbances and these variables are estimated by the separate algorithms, described below.

Model-I is used for the UAV state and disturbances estimation inside the intervals between the corrections based on GNSS signals. In compliance with the given above list of sensors, output vector y_I of this model can be taken as $y_I = \mathrm{col}\{\omega_x, \omega_y, \omega_z, h, \vartheta, \gamma, \psi,\ j_x,\ j_y, j_z\}$. Measurable input vector is taken as $u_I = \mathrm{col}\{\delta_e, \delta_r, \delta_a, \hat{V}_k\}$, where $\hat{V}_k$ stands for the velosity estimate, obtained by means of the extrinsic algorithm.

Thus, the state-space equations of the Model-I $\dot{x}_I(t) = A_I x_I(t) + B_I u_I(t)$, $y_I(t) = C_I x_I(t) + D_I u_I(t)$ have matrices A_I, B_I, C_I, D_I in the following block form:

$$\begin{aligned}
A_I &= \left[\begin{array}{c|c} A_{2,\ldots,12} & B_{(2,\ldots,12),(4,5,6)} \\ \hline & \\ \multicolumn{2}{c}{\mathbf{0}_{3\times 14}} \end{array}\right] \in \mathbb{R}^{14\times 14}, \\
B_I &= \left[\begin{array}{c|c} B_{(2,\ldots,12),(1,2,3)} & A_{(2,\ldots,12),1} \\ \hline & \\ \multicolumn{2}{c}{\mathbf{0}_{3\times 4}} \end{array}\right] \in \mathbb{R}^{14\times 3}, \\
C_I &= \Big[C_{(4,5,6,8,10,11,12,15,16,17),(2,\ldots,12)} \ \Big| \\
&\qquad D_{(4,5,6,8,10,11,12,15,16,17),(4,5,6)}\Big] \in \mathbb{R}^{10\times 14}, \\
D_I &= \Big[D_{(4,5,6,8,10,11,12,15,16,17),(1,2,3)} \ \Big| \\
&\qquad C_{(4,5,6,8,10,11,12,15,16,17),1}\Big] \in \mathbb{R}^{10\times 3},
\end{aligned} \tag{2}$$

where indices show the numbers of the rows and columns of the elements of corresponding matrices of the linearized model that are used in Model-I. The "shift" φ_I for this model is found as

$$\varphi_I = \left[\begin{array}{c} f(x^*, u^*)_{\ 2,\ldots,12} \\ \hline \mathbf{0}_{3\times 1} \end{array}\right] - A_I \left[\begin{array}{c} {x^*}_{2,\ldots,12} \\ \hline \mathbf{0}_{3\times 1} \end{array}\right] - B_I \left[\begin{array}{c} {u^*}_{1,2,3} \\ \hline x_1^* \end{array}\right] \in \mathbb{R}^{14}.$$

Model-II is used for computation of the Kalman estimator feedback gain matrix. It has to satisfy the observability condition and only measurable outputs can be used in this model and only observable states can be estimated. It should be mentioned that Model-II, as itself, is not destined for getting the state estimates. It is used only in order to obtain the estimator feedback gain matrix. There-

fore, this model can be obtained by decomposition into the observable/unobservable subspaces (or, in the other words, by transformation to the Observability Staircase Form). For the considered problem the matrices of Model-II state-space equations can be written as follows:

$$A_{II}=\left[\begin{array}{c|c} A_{2,4,5,6,8,10,11,12} & B_{(2,4,5,6,8,10,11,12),(4,5,6)} \\ \hline \multicolumn{2}{c}{\mathbf{0}_{3\times 11}} \end{array}\right]\in\mathbb{R}^{11\times 11},$$

$$B_{II}=\left[\begin{array}{c} B_{(2,4,5,6,8,10,11,12),(1,2,3)} \\ \hline \mathbf{0}_{3\times 3} \end{array}\right]\in\mathbb{R}^{11\times 3},$$

$$C_{II}=\Big[C_{(4,5,6,8,10,11,12,15,16,17),(2,4,5,6,8,10,11,12)}\,|\, D_{(4,5,6,8,10,11,12,15,16,17),(4,5,6)}\Big]\in\mathbb{R}^{10\times 11},$$

$$D_{II}=\Big[D_{(4,5,6,8,10,11,12,15,16,17),(1,2,3)}\Big]\in\mathbb{R}^{10\times 3}. \quad (3)$$

Sampling. Data processing in the considered systems has a discrete mode, so the discrete-time models have to be found. Assuming the input signal $u(t)$ be constant between the sampling instants $t_k = kT_s$ $(k = 0, 1, 2, \ldots)$, one gets the following discrete-time form of the linearized model:

$$x[k+1]=Px[k]+Qu[k]+T_s\varphi,\quad y[k]=Cx[k]+Du[k], \quad (4)$$

and for the ideal case takes place: from $u[k] \equiv u(t_k)$ and $x[0] = x(t_0)$ follows that $x[k] \equiv x(t_k)$ and $y[k] \equiv y(t_k)$. The P and Q matrices in (4) satisfy the following expressions: $P = \exp(AT_s)$, $Q = \left(\int\limits_0^{T_s} \exp(A\tau)d\tau\right) B$.

Applying this procedure to the Models-I,II, one gets them in form of the difference equations, respectively:

$$\begin{array}{r} \text{Model-I/D: } x_I[k+1] = P_I x_I[k] + Q_I u[k] + T_s\varphi, \\ y_I[k] = C_I x_I[k] + D_I u[k], \end{array} \quad (5)$$

$$\begin{array}{r} \text{Model-II/D: } x_{II}[k+1] = P_{II} x_I[k] + Q_{II} u[k], \\ y_{II}[k] = C_{II} x_{II}[k] + D_{II} u[k], \end{array} \quad (6)$$

where $P_i = \exp(A_i T_s)$, $Q_i = \int_0^{T_s} \exp(A_i\tau)d\tau \cdot B_i$, i=I,II. The state, output and input vectors of these models have the following components:

$x_I = \mathrm{col}\{\theta, \Psi, \omega_x, \omega_y, \omega_z, x, h, z, \vartheta, \gamma, \psi, W_x, W_y, W_z\} \in \mathbb{R}^{14}$,
$y_I = y_{II} = \mathrm{col}\{\omega_x, \omega_y, \omega_z, h, \vartheta, \gamma, \psi, j_x, j_y, j_z\} \in \mathbb{R}^{10}$,
$x_{II} = \mathrm{col}\{\theta, \omega_x, \omega_y, \omega_z, h, \vartheta, \gamma, \psi, W_x, W_y, W_z\} \in \mathbb{R}^{11}$,
$u_I = \mathrm{col}\{\delta_\mathrm{e}, \delta_\mathrm{r}, \delta_a, \hat{V}_k\} \in \mathbb{R}^4$, $\quad u_{II} = \mathrm{col}\{\delta_\mathrm{e}, \delta_\mathrm{r}, \delta_a\} \in \mathbb{R}^3$.

Estimator parameters computation. Discrete full-order state estimator (Kalman Estimator, State Observer) for the plant model $x[k+1] = Px[k] + Qu[k]$, $y[k] = Cx[k] + Du[k]$ is as follows:

$$\begin{array}{l} \hat{x}[k+1] = P\hat{x}[k] + Qu[k] + L[k](y[k] - \hat{y}[k]), \\ \hat{y}[k] = C\hat{x}[k] + Du[k], \end{array} \quad (7)$$

where $\hat{x}[k]$ denotes the estimate of the plant state vector $x(t_k)$ at the kth instant (for real-time systems, $t_k = kT_s$, T_s is a sample time). The problem of the estimator design lies in finding the appropriate gain matrix function $L[k] \in \mathbb{R}^{n\times m}$. In the steady-state mode (after the transient behavior is finished), $L[k] \equiv L$ is a constant matrix gain. The statistical-optimal solution with respect to white-noise disturbances can be found by solving the Riccati equation and turns estimator (7) into the optimal Kalman filter. Optimal filtering application implies sufficiently exact knowledge of the plant model, sensor parameters and disturbance properties. Another approach to estimator design based on the criterion "stability/trancient time" and consists in ensuring the prescribed eigenvalues of estimator (7). This approach is used at the present paper. For the discrete-time systems it is convenient to find the desired eigenvalues z_i (i=1,2,...,n) by transformation $z_i = \exp(p_i T_s)$, where p_i are appropriately picked eigenvalues for a continuous-time system. The estimator transient time t_est can be approximately found as $t_\mathrm{est} \approx 5/\eta$, where $\eta = \min\limits_{i=1,\ldots,n}(-\mathrm{Re}\, p_i)$. The greater η is taken, the greater speed of acting and measurement noise sensitivities are, at the same time the less disturbance and parametristic sensitivities are achieved. In this study are taken $p_i = -\omega_\mathrm{est}(1 + i/n_{II})$, where $\omega_\mathrm{est} > 0$ is the picked estimator parameter, $n_{II} = \dim x_{II} = 11$ is the Model-II (6) degree, $i = 1, 2, \ldots, n_{II}$.

Thus, estimator (7) gain matrix $L \equiv L_{II}$ for plant model (6) should satisfy the following expressions:

$$z_i = \exp(p_i T_s),\ \ \det(z_i \mathbf{I}_{n_{II}} - P_{II} + L_{II} C_{II}) = 0, \quad (8)$$

where $\mathbf{I}_{n_{II}}$ denotes the identity $n_{II} \times n_{II}$ matrix, $i = 1,\ldots,n_{II}$. To find matrix L_{II}, the duality theorem and pole placement technique (Kautsky et al., 1985) may be used.

After the gain matrix L_{II} is found, it is used for designing the real-time estimator, based on the Model-I (2). A modification is made for fitting the estimator algorithm to the nonlinear UAV model (Chen et al., 2009; Ye et al., 2006): the estimator output $\hat{y}_I$ is calculated from the *nonlinear* relation $\hat{y}_I = g(\hat{x}_I, u_I)$. Therefore, the acceleratons are found as

$$\begin{array}{l} j_x = -g\sin\hat{\vartheta} + (P\cos\varphi - \hat{X})/m, \\ j_y = -g\cos\hat{\vartheta}\cos\hat{\gamma} + (P\sin\varphi + \hat{Y})/m, \\ j_z = g\cos\hat{\vartheta}\sin\hat{\gamma} + \hat{Z}/m, \end{array}$$

where $\hat{\vartheta}, \hat{\gamma}$ are the estimates of the angles ϑ, γ; $\hat{X}, \hat{Y}, \hat{Z}$ denote the estimates of the stopping, lift and lateral forces, obtained on the base of estimation $\hat{x}_I$ of the vehicle state vector x_I. Finally, the discrete-time state estimator is as follows:

$$\begin{array}{l} \hat{x}_I[k+1] = P_I\hat{x}_I[k] + Q_I u_I[k] + L_I(y_I[k] - \hat{y}_I[k]), \\ \hat{y}_I[k] = g(\hat{x}_I[k], u_I[k]). \end{array} \quad (9)$$

The rows of 14×10-matrix L_I should be copied from those of matrix L_{II}. The rest elements of matrix L_{II} are zeros.

Given above method of the estimator design can be treated as a row of the successive steps: separation of the plant model into the observable and unobservable subsystems; the estimator design for the observable subsystem; return to the original model.

Estimator state renewal. As it is told above, it the instants t_K of the GNSS availability re-counting of some estimates should be fulfilled. Renewing procedure of the estimator state is as follows:

$$\hat{x}[k_r] = x^{GNSS}(t_K), \quad \hat{h}[k_r] = h^{GNSS}(t_K),$$
$$\hat{z}[k_r] = z^{GNSS}(t_K), \quad \hat{V}_k[k_r] = V_k^{GNSS}(t_K),$$

where $k_r = \mathrm{E}(t_K/T_s)$ are the discrete-time instants, corresponding to t_K; $E(\cdot)$ stands for the integral part function; $x^{GNSS}, h^{GNSS}, z^{GNSS}(t_K), V_k^{GNSS}$ are obtained by means of primary data processing of the GNSS signals.

Supplementary estimation. The estimates of V_k and Ψ, embedded into the similar estimation procedure turned out to be very sensitive to the measurement noise and disturbances. Therefore the other algorithms are used for estimation of these variables. The value of V_k between the instants t_K is estimated via the discrete-time integration of the accelerometer signal j_x:

$$\hat{V}_k[k+1] = \hat{V}_k[k] + T_s\, j_x[k], \quad j_x[k] = j_x(t_k), \quad t_k = k\,T_s \qquad (10)$$

Estimates $\hat{\Psi}$ of the track angle Ψ inside the time intervals $[t_{K-1}, t_K)$ are obtained via estimator (9) with no correction by the feedback signal (note, that all elements of matrix L_I are equal to zero in the corresponding row). At the instants t_K for renewal of $\hat{\Psi}$ the equation $\dot{z} = -V_k \sin\Psi\cos\theta$. Assuming $\Psi(t)$ to be constant for $t \in [t_{K-1}, t_K]$ (i.e. $\Psi(t) \equiv \Psi(t_K)$ for $t_K \le t < t_{K+1}$),one gets the following formula for $\hat{\Psi}$ correction at the instants t_K:

$$\hat{\Psi}(t_K) = -\arcsin \frac{z(t_{K+1}) - z(t_K)}{\int_{t_K}^{t_{K+1}} V_k(t)\theta(t)dt}.$$

Finally, commuting $V_k(t), \theta(t)$ into their discrete-time estimates $\hat{V}_k[k], \hat{\theta}[k]$ from (9) and having used finite summation instead of integration, one obtains the following renewal algorithm:

$$\hat{\Psi}(t_K) = -\arcsin \frac{z^{GNSS}(t_K) - z^{GNSS}(t_{K-1})}{T_s \sum_{i=0}^{N_S-1} \hat{V}_k[N+i]\hat{\theta}[N+i]}, \quad (11)$$

where $N_S = E\left(\frac{t_K - t_{K-1}}{T_s}\right)$, $N = E\left(\frac{t_{K-1}}{T_s}\right)$.

Formulas (9), (10), (11) present the proposed UAV state estimation algorithm with the GNSS corrections.

3.1 Numerical analysis of the UAV flight parameters estimation

In this Section some numerical results of efficiency and accuracy of the navigation algorithm, proposed in the Section 3 are given. The UAV model is taken in the form of (Chen et al., 2009; Ye et al., 2006). Let the following mass/geometrical parameters of the hypothetical UAV be taken: length, $L = 2.31$ m; diameter, $D = 0.152$ m; wing-span, $l_k = 0.8$ m; wing aspect ratio, $\lambda_k = 5$; wing surface area, $S_k = 0.128$ m^2; UAV cruising mass, $m = 38.5$ kg; cruising speed, $V = 250$ m/s; cruising thrust, $P = 225$ N; moments of inertia,[2] $J_x = 0.162$, $J_y = 13.7$, $J_z = 13.7$ kg·m^2. For the numerical example the linearized UAV model is found with regard to the reference state $x^* = \mathrm{col}\{250, 0, 0, 0,\ 0, 0,\ 0, 6000, 0, 0.0337, 0, 0\}$, $u^* = \mathrm{col}\{-0.209, 0, 0, 0, 0, 0, 0\}$. The picked values of $V_k^*, h^*, \vartheta^*, \delta_{\mathrm{r}}^*$ are near to those of the balancing (trimmed) level flight. The thrust nominal value P^* is taken as $P^* = 221$ N.

Simulation parameters. At this phase of resarch the main attention is paid to data processing for navgation. The considered UAV possesses arrow stability and the open loop system is simulated with the initial state $x_0 = \mathrm{col}\{235, 0, -0.087, 0, 0, 0, 0, 6000, 0, 0.035, 0, \ -0.0785\}$ and constant rudder deflections: $\delta_{\mathrm{e}} = -0.209, \delta_a = \delta_{=}0$ rad. The estimator initial state is taken as $x_{0_{\mathrm{est}}} = \mathrm{col}\{250, 0, -0.077, 0, 0, 0, 0, 6000, 0, 0.033, 0, -0.0785\}$ The thrust is assumed to be nominal, $P = 221$ N. For a start, all the sensors and the GNSS position/velocity data are supposed to be ideal. The aim of the presented below results is to ascertain the dynamical properties of the estimator, the effects of wind disturbances and vanishing the GNSS signal. The atmospheric wind simulation is a difficult independent problem (see, for example, (Hedin et al., 1988, 1996; Anonymous, 1954)). In this simulation the simplified wind model is taken: components W_x, W_y, W_z of the wind velocity vector are taken as the stationary stochastic processes with mean values $\{10, -17, 7\}$ m/s (respectively), and self-correlated functions $R(\tau) = \sigma^2 \exp(-\mu|\tau|)$, $\sigma = 10$ m/s, $\mu = 0.3$ 1/s. The sample time T_S for the GNSS data processing is assummed to be constant, $T_S = 5$ s. The estimator parameter $\omega_{\mathrm{est}} = 2.5$ s^{-1} is taken.

The ideal measurements The simulation was made by MATLAB^R 5 – SIMULINK software. Some results are shown in Fig. 1–2.

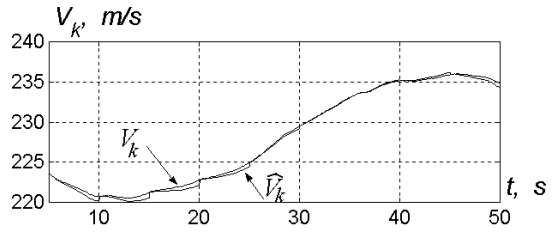

Fig. 1. Velosity V_k Estimation.

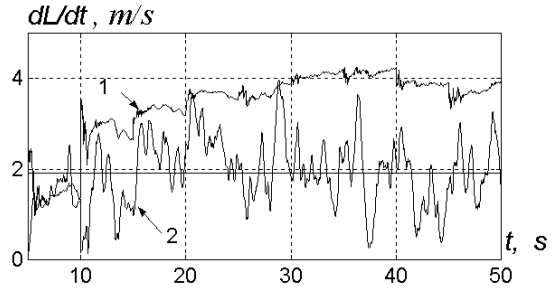

Fig. 2. Rate of Position Estimation Error.

Statistical properties of the estimation errors are presented in Table 3.1.2.

In Fig. 2 the rate of error between the real and estimated UAV positions is shown (curve 1). This curve was obtained by numerical time-differentiation of the deviation vector between the real UAV position (x, h, z) and its estimated value $(\hat{x}, \hat{h}, \hat{z})$: $L(t) = \sqrt{(x-\hat{x})^2 + (h-\hat{h})^2 + (z-\hat{z})^2}$.

[2] Some of the UAV parameters (the weight, moments of inertia) are changing during the flight; their nominal values for the considered flight conditions are presented.

Table 1. Statistical properties of the estimation errors.

	ΔV_k, m/s	$\Delta\theta$, rad	$\Delta\Psi$, rad	ΔW_x, m/s	ΔW_y, m/s	ΔW_z, m/s
Mean M	0.1	$-7.6\cdot10^{-3}$	$8.7\cdot10^{-4}$	-0.11	-1.3	-0.12
Std, σ	0.24	$4.1\cdot10^{-3}$	$2.1\cdot10^{-3}$	1.1	2.1	1.4

This curve shows, that the position error $L(t)$ increases with the rate about 4 meters per every second, when GNSS is unavailable. The curve 2 shows the better accuracy; the mean value of $\dot{L}$ is about 2 m/s. This curve was found through the difference between the real $\mathbf{V}_k$ and estimated $\hat{\mathbf{V}}_k$ UAV velocity vectors, namely: $\mathbf{V}_k = \mathrm{col}\{V_k\cos\theta\cos\Psi, V_k\sin\theta, -V_k\sin\Psi\cos\theta\}$, $\hat{\mathbf{V}}_k = \mathrm{col}\{\hat{V}_k\cos\hat{\theta}\cos\hat{\Psi}, \hat{V}_k\sin\hat{\theta}, -\hat{V}_k\sin\hat{\Psi}\cos\hat{\theta}\}$, $\dot{L} = \|\mathbf{V}_k - \hat{\mathbf{V}}_k\|$. In short, position estimates have greater errors, than would be achieved via the velocity integration. The reason of this effect lies in the linearity of the estimator (9) equation. Hence, to improve the estimation accuracy, let us modify the algorithm (9), bringing the nonlinear relations on the estimator equations.

Nonlinear estimator. Let us use the nonlinear model of the UAV translational kinematics. Similarly to (10), one gets the following discrete-time recurring algorithm:

$$\begin{aligned}\hat{x}[k+1] &= \hat{x}[k] + T_s\,\hat{V}_k[k]\cos(\hat{\theta}[k])\cos(\hat{\Psi}[k]),\\ \hat{h}[k+1] &= \hat{h}[k] + T_s\,\hat{V}_k[k]\sin(\hat{\theta}[k]) + L_h e[k],\\ \hat{z}_k[k+1] &= \hat{z}[k] - T_s\,\hat{V}_k[k]\cos(\hat{\theta}[k])\sin(\hat{\Psi}[k]).\end{aligned} \qquad (12)$$

This algorithm should be used instead of the linear one in (10) on the steps between the GNSS corrections in the instants t_r. Term $L_h e[k]$ in the formula for $\hat{h}$ appears as a corresponding row of $L(y[k] - \hat{y}[k])$, in the estimator (9) ($e[k]$ denotes $y_I[k] - \hat{y}_I[k]$, $L_h \equiv L_{I_7}$ for the considered case with the estimator equation (9)). Finally, the (9) is modified as follows: rows 6,7,8 of matrix Q_I are taken zeros; rows 6,7,8 of matrix P_I are changed as follows: $P_{I_i} = [0,\ldots,0,\overbrace{1}^{i},0,\ldots,0]$, where $i = 6,7,8$;

3. Equations (12) are implemented in the estimation procedure between the corrections from GNSS.

The ideal measurements and nonlinear estimator. Simulation of the system with the nonlinear estimator gives the accuracy characteristics presented in Table 2.

In Fig. 3 the rates of error between the real and estimated UAV positions, analogously those in Fig. 2, are shown. These results demonstrated that the accuracy properties could be improved by means of the nonlinear estimator.

Now let us turn to the study the state estimation accuracy in the presence of measuring errors.

Perturbed measurements and nonlinear estimator. Let us take into account some errors in the sensors/GNSS data, which act on the system in addition to the wind disturbances. The following perturbations model is used: the real value of the thrust $P = 231$ N, for estimation the trust is assumed to be 221 N, $\Delta P = 10$ N; measuring values of the rudders deflection differ from the real ones on the constant shift $\mathbf{\Delta}\delta_{e,r,a} = \{3.5\cdot10^{-3}, -3.5\cdot10^{-3}, -3.5\cdot10^{-3}\}$ rad; GNSS measuring velocity errors ΔV_k^{GNSS} are taken as the Gaussian random numbers with zero mean and the

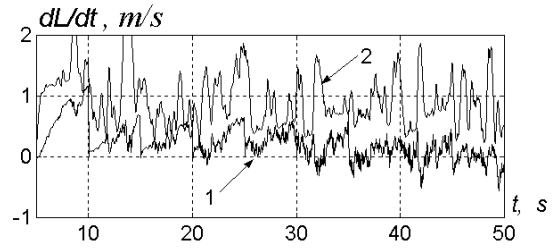

Fig. 3. Rate of Position Estimation Error for Nonlinear Algorithm.

standard deviation $\sigma_{\Delta V} = 0.5$ m/s; GNSS measuring position errors $\Delta x^{GNSS} = \Delta h^{GNSS} = \Delta z^{GNSS} =$ are taken as the Gaussian random numbers with zero mean and the standard deviation $\sigma_{\Delta x,h,z} = 2$ m; rate gyro errors $\mathbf{\Delta}\omega_{x,y,z}$ are taken as the Gaussian random numbers with mean $\{5\cdot10^{-4}, -5\cdot10^{-4}, 5\cdot10^{-4}\}$ rad/s and and the standard deviation $\sigma_{\Delta\omega x,y,z} = 5\cdot10^{-4}$ rad/s; positional gyro errors $\mathbf{\Delta}_{\vartheta,\psi,\gamma} = \{5\cdot10^{-4}, -3\cdot10^{-4}, -5\cdot10^{-4}\}$ rad; altitude errors Δ_{h_a} are taken as the Gaussian random numbers with mean 3 m and the standard deviation $\sigma_{\Delta h_a} = 5$ m; acceleration errors $\mathbf{\Delta j}_{x,y,z}$ are taken as the Gaussian random numbers with mean $\{-0.02, 0.03, 0.02\}$ m/s^2 and the standard deviation $\sigma_{\Delta j} = 0.02$ m/s^2.

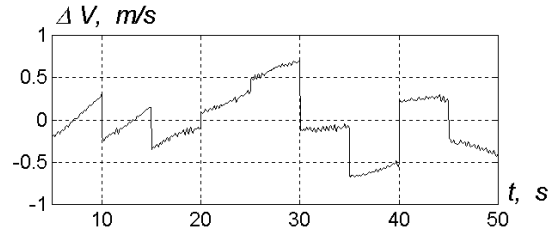

Fig. 4. Velocity Estimation Error.

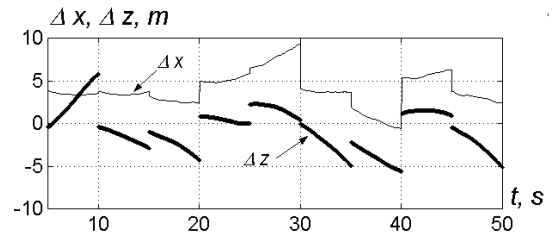

Fig. 5. Position Estimation Errors Δx, Δz .

Simulation results for the considered perturbed system are shown in Figs. 4, 5. Numerical results show that the position error grows with the rate about 2.3 m/s in average between the instants of GNSS corrections.

4. CONCLUSION

The algorithm for UAV position estimation with the onboard sensors and GNSS corrections is proposed and numerically investigated. The future work intensions are as follows: usage of more realistic model of sensor errors,

Table 2. Nonlinear estimation accuracy

	L, m	$\Delta\theta$, rad	$\Delta\Psi$, rad	ΔW_x, m/s	ΔW_y, m/s	ΔW_z, m/s
Mean M	5.0	$2.9 \cdot 10^{-3}$	$9.9{\cdot}10^{-4}$	-0.11	0.56	-0.14
Std, σ	0.54	$3.9{\cdot}10^{-3}$	$3.2{\cdot}10^{-3}$	1.1	1.8	1.5

GNSS primary data processing (Blanch et al., 2008) and wind disturbances; research of the accuracy, achievable by means of the optimal Kalman filtering; usage of the completely nonlinear estimator, which seems to be more adequate to the UAV dynamics for the different flight conditions; investigation of the suitability of the on-line identification methods for tuning the estimator during the flight.

REFERENCES

Algrain, M. and Saniie, J. (1994). Interface Kalman filtering of 3D-angular motion based on Euler's nonlinear equations. *IEEE Trans. Aerosp. Electron. Syst.*, 30(1), 175–185.

Anonymous (1954). Manual of the ICAO standard atmosphere calculations by the NACA. URL `http://naca.central.cranfield.ac.uk/reports/1954/naca-tn-3182.pdf`.

Balluchi, A., Benvenuti, L., Di Benedetto, M.D., and Sangiovanni-Vincentelli, A.L. (2012). The design of dynamical observers for hybrid systems: Theory and application to an automotive control problem. Technical Report, No 1, Sapienza University of Rome, Dep. Computer and System Sci.

Blanch, J., Walter, T., and Enge, P. (2008). Position error bound calculation for GNSS using measurement residuals. *IEEE Trans. Aerosp. Electron. Syst.*, 44(3), 977–984.

Blomenhofer, H. (1996–1997). Accuracy, integrity, and availability of GLS-based autopilot-coupled aircraft landings. *Navigation: Journ. of the ION*, 43(4), 419–435.

Chen, X., Ou, Q., Wong, D.R., Li, Y.J., Sinclair, M., and Marburg, A. (2009). Flight dynamics modelling and experimental validation for unmanned aerial vehicles. In X. Chen (ed.), *Mobile Robots – State of the Art in Land, Sea, Air, and Collaborative Missions*, 177–202. InTech. URL `http://www.intechopen.com/books`.

Coffee, J. and Maganty, P. (1996). An intergrated DGPS/INS navigation system for a ballistic missile: design and flight test results. *Navigation: Journ. of the ION.*, 43(3), 273–294.

Dmitriev, S., Stepanov, O., and Koshaev, D. (1999). Methods of data integration for INS and navigation satellite system. *Gyroscopy and Navigation*, 3(26), 36–52.

Hedin, A., Fleming, E., and Manson, A. (1996). Empirical wind model for the upper, middle and lower atmosphere. *J. Atmos. Terr. Phys.*, 58, 1421–1447.

Hedin, A., Spencer, N., and Killeen, T. (1988). Empirical global model of upper thermosphere winds based on atmosphere and dynamics explorer satellite data. *J. Geophys. Res.*, 93, 9959–9978.

Hegrenaes, O. and Hallingstad, O. (2011). Model-aided INS with sea current estimation for robust underwater navigation. *IEEE J. Oceanic Eng.*, 36(2), 316–337.

Hemsch, M. and Mendenhall, M.R. (1992). *Tactical missile aerodynamics.* AIAA, NASA, Calif., USA.

Kautsky, J., Nichols, N.K., and Van Dooren, P. (1985). Robust pole assignment in linear state feedback. *Int. J. Control*, 41(5), 1129–1155.

Koifman, M. and Bar-Itzhack, I. (1999). Inertial navigation system aided by aircraft dynamics. *IEEE Trans. Contr. Syst. Technol.*, 7(4), 487–493.

Koifman, M., Bar-Itzhack, I., and Mernav, S. (1995). Dynamics aided Inertial Navigation System. In *Proc. AIAA-95-3195-CP. Guidance. – Navigation and Control Conference*, 204–213.

Morgado, M., Oliveira, P., and Silvestre, C. (2013). Tightly coupled ultrashort baseline and inertial navigation system for underwater vehicles: An experimental validation. *Journal of Field Robotics*, 30(1), 142–170.

Mutuel, L. and Speyer, J. (2000). Fault–tolerant INS/GPS navigation system with application to unmanned aerial vehicle. In *Proc. ION GPS 2000 Convention.* Salt Lake City, Utah, USA.

Perera, L., Wijesoma, W., and Adams, M. (2010). SLAM with joint sensor bias estimation: Closed form solutions on observability, error bounds and convergence rates. *IEEE Trans. Contr. Syst. Technol.*, 18(3), 732 – 740.

Sazdovski, V. and Silson, P. (2011). Inertial navigation aided by vision-based simultaneous localization and mapping. *IEEE Sensors J.*, 11(8), 1646–1656.

Strachan, V. (1997). The global positioning system as a sole means of navigation. In *Proc. Civil Avionics '97 Conference.*

Tanju, B., Minarik, S., Falchetti, C., Savage, G., and May, M. (2000). Enhanced link 16/GPS/INS navigation, robust tactical navigation resource for the military. In *Proc. ION GPS 2000 Convention.* Salt Lake City, Utah, USA.

Tanwani, A., Shim, H., and Liberzon, D. (2013). Observability for switched linear systems: Characterization and observer design. *IEEE Trans. Automat. Contr.* (submitted).

Vallot, L., Snyder, S., and Schipper, B. (1991). Design and flight test of a differential GPS/INERTIAS navigation system for approach/landing guidance. *Navigation: Journ. of the ION.*, 38(2), 103–122.

Vasconcelos, J., Silvestre, C., and Oliveira, P. (2011). INS/GPS aided by frequency contents of vector observations with application to autonomous surface crafts. *IEEE J. Oceanic Eng.*, 36(2), 347 – 363.

Vasconcelos, J., Silvestre, C., Oliveira, P., and Guerreiro, B. (2010). Embedded UAV model and LASER aiding techniques for inertial navigation systems. *Control Engineering Practice*, 18(3), 262 – 278.

Ye, Z., Bhattacharya, P., Mohamadian, H., Majlesein, H., and Ye, Y. (2006). Equational dynamic modeling and adaptive control of uav. In *System of Systems Engineering, 2006 IEEE/SMC International Conference on*, 5. doi:10.1109/SYSOSE.2006.1652318.